J|A|C|S ARTICLES

Published on Web 02/05/2010

Glycodynamers: Dynamic Polymers Bearing Oligosaccharides Residues − Generation, Structure, Physicochemical, Component Exchange, and Lectin Binding Properties

Yves Ruff,[†] Eric Buhler,[‡] Sauveur-Jean Candau,[†] Ellina Kesselman,[§] Yeshayahu Talmon,[§] and Jean-Marie Lehn*[,†]

Laboratoire de Chimie Supramoléculaire, ISIS, Université de Strasbourg, Allée Gaspard Monge, 67000 Strasbourg, France, Laboratoire Matière et Systèmes Complexes (MSC), UMR CNRS 7057, Bâtiment Condorcet, Université Paris Diderot-Paris 7, 75205 Paris cedex 13, France, and Department of Chemical Engineering, Technion-Israel Institute of Technology, Haifa 32000, Israel

Received October 7, 2009; E-mail: lehn@isis.u-strasbg.fr

Abstract: Dynamic glycopolymers have been generated by polycondensation through acylhydrazone formation between components bearing lateral bioactive oligosaccharide chains. They have been characterized as bottlebrush type by cryo-TEM and SANS studies. They present remarkable fluorescence properties whose emission wavelengths depend on the constitution of the polymer and are tunable by constitutional modification through exchange/incorporation of components, thus also demonstrating their dynamic character. Constitution-dependent binding of these glycodynamers to a lectin, peanut agglutinin, has been demonstrated.

Constitutional dynamic chemistry (CDC)[1] rests on the implementation of reversible chemical connections of either covalent or noncovalent nature linking the components of a molecular or supramolecular entity. As a consequence, constitutionally dynamic entities are able to continuously modify their constitution by assembly disassembly of their building blocks, thus generating a mixture of interconvertible species, a dynamic set of constituents, a constitutional dynamic library[1] (CDL).

A CDL is also combinatorial, as all possible combinations of the initial building blocks may form in proportions specific to the thermodynamic equilibrium of the system.[2−4] Disruption of this equilibrium by physical or chemical factors may lead to adaptation through amplification of one or more constituents of the library by rearrangement of its components. This approach was used successfully, for example, for the discovery of biologically active substances selected by the biological target itself under the pressure of recognition.[5]

The implementation of CDC in material science, in particular in polymer chemistry, led to the introduction of the notion of dynamic polymers, dynamers that result from the reversible connection of monomers via either covalent or noncovalent linkages.[6−8] Such equilibrium polymers present the ability to undergo changes in their constitution, length, and sequence even after polymerization. These modifications can be triggered by physical stimuli or chemical effectors like temperature,[8] or addition of protons[9] or of metal cations.[10−12] Dynamers are thus smart, adaptive materials. Moreover, changes in the molecular constitution of the polymer can induce a modification of the properties (such as mechanical[13] or optical[10,12,14]) of the material.

Dynamers based on components of biological nature may generate dynamic analogues of natural polymers, *biodynamers*, that offer the possibility to combine the functional properties (recognition, catalysis) of naturally occurring polymers with the adaptive behavior of constitutional dynamic systems. Therefore, in view of the prospects offered, the incorporation of biologically relevant moieties into dynamic polymers deserves close scrutiny.[15−18]

In addition to proteins and nucleic acids, polysaccharides represent a third class of biopolymers. Oligo- and polysaccharides are involved in a wide range of biological or pathological events like immune response, inflammation, cancer, cell adhe-

[†] Université de Strasbourg.
[‡] Université Paris Diderot-Paris 7.
[§] Technion-Israel Institute of Technology.

(1) Lehn, J.-M. *Chem. Soc. Rev.* **2007**, *36*, 151–160.
(2) Rowan, S. J.; Cantrill, S. J.; Cousins, G. R. L.; Sanders, J. K. M.; Stoddart, J. F. *Angew. Chem., Int. Ed.* **2002**, *41*, 898–952.
(3) Corbett, P. T.; Leclaire, J.; Vial, L.; West, K. R.; Wietor, J.-L.; Sanders, J. K. M.; Otto, S. *Chem. Rev.* **2006**, *106*, 3652–3711.
(4) Lehn, J.-M. *Chem.-Eur. J.* **1999**, *5*, 2455–2463.
(5) Ramström, O.; Lehn, J.-M. *Nat. Rev. Drug Discovery* **2002**, *1*, 26–36.
(6) Lehn, J.-M. *Prog. Polym. Sci.* **2005**, *30*, 814–831.
(7) Lehn, J.-M. *Polym. Int.* **2002**, *51*, 825–839.
(8) Yamaguchi, G.; Higaki, Y.; Otsuka, H.; Takahara, A. *Macromolecules* **2005**, *38*, 6316–6320.
(9) Ono, T.; Nobori, T.; Lehn, J.-M. *Chem. Commun.* **2005**, 1522–1524.
(10) Giuseppone, N.; Lehn, J.-M. *J. Am. Chem. Soc.* **2004**, *126*, 11448–11449.
(11) Fujii, S.; Lehn, J.-M. *Angew. Chem., Int. Ed.* **2009**, *48*, 7635–7638.
(12) Giuseppone, N.; Fuks, G.; Lehn, J.-M. *Chem.-Eur. J.* **2006**, *12*, 1723–1735.
(13) Ono, T.; Fujii, S.; Nobori, T.; Lehn, J.-M. *Chem. Commun.* **2007**, 46–48.
(14) Ono, T.; Fujii, S.; Nobori, T.; Lehn, J.-M. *Chem. Commun.* **2007**, 4360–4362.
(15) Nakazawa, I.; Suda, S.; Masuda, M.; Asai, M.; Shimizu, T. *Chem. Commun.* **2000**, 881–882.
(16) Sreenivasachary, N.; Hickman, D. T.; Sarazin, D.; Lehn, J.-M. *Chem.-Eur. J.* **2006**, *12*, 8581–8588.
(17) Ruff, Y.; Lehn, J.-M. *Biopolymers* **2008**, *89*, 486–496.
(18) Ruff, Y.; Lehn, J.-M. *Angew. Chem., Int. Ed.* **2008**, *47*, 3556–3559.

sion, or cell−cell recognition.[19−21] These recognition processes involve in particular carbohydrate−protein interactions. As the interaction of a single saccharide with its receptor is generally weak, biology uses multivalency to enhance the binding efficiency.[22] The oligosaccharides involved in recognition processes are generally clustered, displayed in a multivalent fashion, at the surface of cells or bacteria.[23] It is therefore of much interest to design synthetic analogues of these natural multivalent assemblies to mimic, or even improve over, their native properties.[24]

One possible approach consists of conjugating carbohydrate residues to a polymerizable scaffold.[25] Glycoclusters have been obtained by appending saccharide residues to branched[26] or hyperbranched polymers,[27] β-cyclodextrin,[28,29] and calixarene cores.[30] Other approaches involve, for instance, combinatorial glycosamino acids[31] and oligosaccharide[32] derivatives, dynamic monolayers,[33] a polyrotaxane,[34,35] and self-assembling glycodendrimers.[36]

Extending our work on dynamers[6,7] to the biopolymer area,[16−18] we were interested in designing dynamic analogues of glycopolymers, *glycodynamers*. Such dynamic or equilibrium polymers could provide, in addition to potential biorecognition properties, an adaptive character that would enable them to reorganize their sequence or constitution so as to select the preferential/optimal sequence, nature, and proportion of the bioactive monomeric subunits, in response to external physical stimuli or chemical effectors (temperature, pH, etc.) or to the presence of a (bio)chemical target template.

Such biodynamers may be of three types: (1) main chain, resulting from polycondensation of saccharide residues through reversible reactions; (2) side chain, where the saccharide residues are either (a) appended on a dynamic main chain or (b) reversibly grafted on a nondynamic main chain; and (3) "doubly dynamic", incorporating both main-chain and side-chain dynamics.

Of special interest, as reversible condensation reaction, is the formation of an imine-type double bond from an amino group and a carbonyl group. Thus, oxime formation has been used in the preparation of dynamic analogues of oligoarabinofuranoses,[17] multiple saccharide presentation,[37−39] and in glycoblotting.[40]

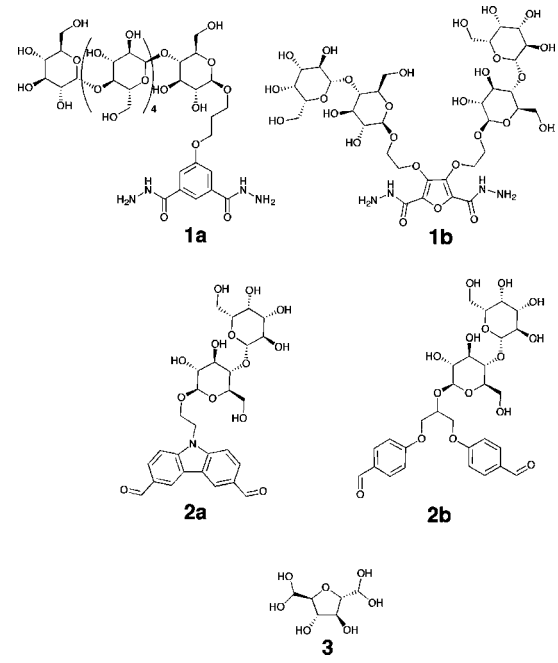

Figure 1. Molecular structures of the bis-hydrazides **1a**,**b** and of the dialdehydes **2a**,**b** and **3**.

Polymers incorporating carbohydrate-based monomers have been obtained by poly(acylhydrazone)[41,42] and polyoxime[43] formation. Ditopic saccharide monomers yield reversible polymers with a bis-boronic acid,[15] and a dynamic library of cyclic sugar oligomers has been generated via acylhydrazone formation.[44]

We present here our results on the generation of glycodynamers of type (2)(a) (vide supra), that is, a nonglycosydic dynamic main chain bearing lateral carbohydrate residues. We also report their remarkable physical and optical properties, the dynamic modulation of the latter, as well as their constitution-dependent binding to a lectin.

Molecular Design of the Monomers

The monomers **1**−**3** were chosen so as to contain structurally diverse aromatic cores to ensure a wide range of properties for the different monomer combinations, allowing one to follow the polymer compositions by various spectroscopic methods such as NMR, UV, or fluorescence spectroscopy.

The starting monomers consist of aromatic bis-hydrazide **1a**, **1b**, and dialdehyde **2a**, **2b**, decorated by oligosaccharide groups

(19) Dube, D. H.; Bertozzi, C. R. *Nat. Rev. Drug Discovery* **2005**, *4*, 477–488.
(20) Shriver, Z.; Raguram, S.; Sasisekharan, R. *Nat. Rev. Drug Discovery* **2004**, *3*, 863–873.
(21) Rudd, P. M.; Elliott, T.; Cresswell, P.; Wilson, I. A.; Dwek, R. A. *Science* **2001**, *291*, 2370–2376.
(22) Mathai Mammen, S.-K. C.; George Whitesides, M. *Angew. Chem., Int. Ed.* **1998**, *37*, 2754–2794.
(23) Lundquist, J. J.; Toone, E. J. *Chem. Rev.* **2002**, *102*, 555–578.
(24) Houseman, B.; Mrksich, M. *Top. Curr. Chem.* **2002**, *218*, 1–44.
(25) Ladmiral, V.; Melia, E.; Haddleton, D. M. *Eur. Polym. J.* **2004**, *40*, 431–449.
(26) Narumi, A.; Kakuchi, T. *Polym. J.* **2008**, *40*, 383–397.
(27) Papp, I.; Dernedde, J.; Enders, S.; Haag, R. *Chem. Commun.* **2008**, 5851–5853.
(28) Smiljanic, N.; Moreau, V.; Yockot, D.; García Fernández, J.; Djedaïni-Pilard, F. *J. Inclusion Phenom. Macrocycl. Chem.* **2007**, *57*, 9–14.
(29) Fulton, D. A.; Stoddart, J. F. *Org. Lett.* **2000**, *2*, 1113–1116.
(30) Aoyama, Y. *Chem.-Eur. J.* **2004**, *10*, 588–593.
(31) Schweizer, F. *Angew. Chem., Int. Ed.* **2002**, *41*, 230–253.
(32) Yamago, S.; Yamada, T.; Ito, H.; Hara, O.; Mino, Y.; Yoshida, J.-i. *Chem.-Eur. J.* **2005**, *11*, 6159–6174.
(33) Yeo, W.-S.; Yousaf, M. N.; Mrksich, M. *J. Am. Chem. Soc.* **2003**, *125*, 14994–14995.
(34) Nelson, A.; Stoddart, J. F. *Org. Lett.* **2003**, *5*, 3783–3786.
(35) Nelson, A.; Belitsky, J. M.; Vidal, S.; Joiner, C. S.; Baum, L. G.; Stoddart, J. F. *J. Am. Chem. Soc.* **2004**, *126*, 11914–11922.
(36) Thoma, G.; Streiff, M. B.; Katopodis, A. G.; Duthaler, R. O.; Voelcker, N. H.; Ehrhardt, C.; Masson, C. *Chem.-Eur. J.* **2006**, *12*, 99–117.
(37) Renaudet, O.; Dumy, P. *Org. Lett.* **2003**, *5*, 243–246.
(38) Singh, Y.; Renaudet, O.; Defrancq, E.; Dumy, P. *Org. Lett.* **2005**, *7*, 1359–1362.
(39) Renaudet, O.; Dumy, P. *Org. Biomol. Chem.* **2006**, *4*, 2628–2636.
(40) Shimaoka, H.; Kuramoto, H.; Furukawa, J.-i.; Miura, Y.; Kurogochi, M.; Kita, Y.; Hinou, H.; Shinohara, Y.; Nishimura, S.-I. *Chem.-Eur. J.* **2007**, *13*, 1664–1673.
(41) Roberts, G. A. F.; Thomas, I. M. *Makromol. Chem.* **1981**, *182*, 2611–2617.
(42) Kirker, K. R.; Luo, Y.; Nielson, J. H.; Shelby, J.; Prestwich, G. D. *Biomaterials* **2002**, *23*, 3661–3671.
(43) Andreana, P. R.; Xie, W.; Cheng, H. N.; Qiao, L.; Murphy, D. J.; Gu, Q.-M.; Wang, P. G. *Org. Lett.* **2002**, *4*, 1863–1866.
(44) Bornaghi, L. F.; Wilkinson, B. L.; Kiefel, M. J.; Poulsen, S.-A. *Tetrahedron Lett.* **2004**, *45*, 9281–9284.

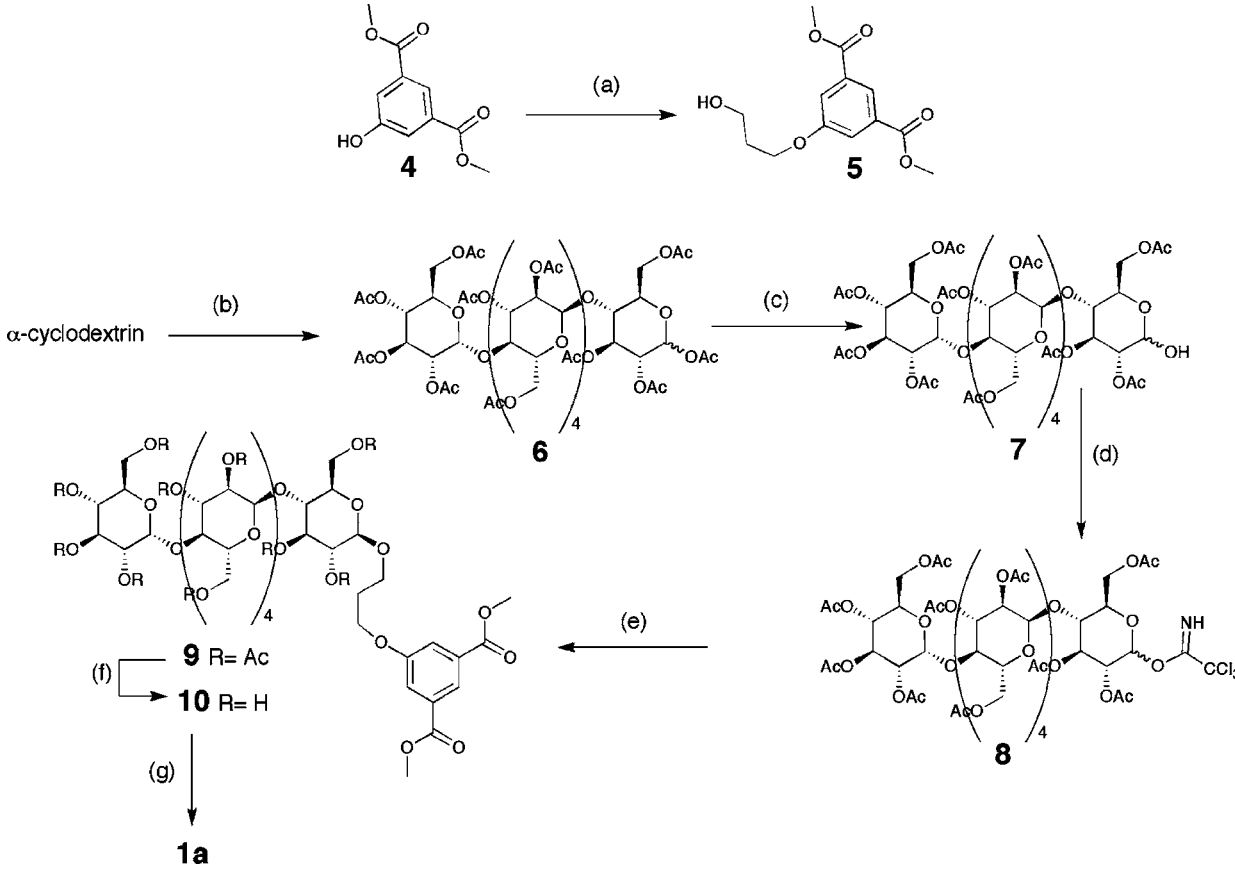

Figure 2. Synthesis of monomer **1a**: (a) 1,3 propanediol, PPh_3, DIAD, THF, 67%; (b) (i) I_2, Ac_2O, (ii) $HClO_4$, Ac_2O, quant.; (c) piperidine, THF, 70%; (d) trichloroacetonitrile, DBU cat., CH_2Cl_2, 64%; (e) **5**, BF_3OEt_2, CH_2Cl_2, −20 °C, 39.5%; (f) KCN, MeOH, 67%; (g) NH_2NH_2 monohydrate, MeOH, 68%.

(Figure 1). Monomer **1a** bears the maltohexaose moiety, derived from α-cyclodextrin, chosen to confer a well-defined secondary structure to the resulting polymer. Such a long hydrophilic side chain conjugated to an hydrophobic aromatic main chain could be expected to result in the formation of a bottlebrush-like species,[45] similar to a cylindrical micelle that would be stabilized via reversible covalent bonds.

Monomers **1b**, **2a**, and **2b** present the lactose moiety that is one of the natural ligands for galectins. These carbohydrate-binding proteins are involved in cell adhesion, inflammation, and cancer.[46,47] Therefore, tools for profiling or binding this type of lectins are needed to understand their biological functions. Furthermore, lactosyl and galactosyl glycopolymers have applications for Shiga toxin 1 binding,[48] and cell-specific gene[49−51] or drug delivery,[52,53] due to their ability to use lectin binding to enhance endocytosis.

Materials and Methods

Materials Synthesis. The synthesis[54] of **1a** starts with the acetolytic cleavage of α-cyclodextrin, followed by a selective deprotection of the anomeric hydroxyl group of **6** giving **7** and activation of the resulting free alcohol to yield the glycosyl donor **8**. **8** is then subjected to a glycosylation using Schmidt's method with the alcohol **5**, which was itself obtained by a Mitsunobu reaction between **4** and 1,3-propandiol. Deprotection of **9** followed by reaction with hydrazine gave **1a** (Figure 2).

The synthesis of dialdehyde **2b** involved the $BF_3 \cdot OEt_2$-catalyzed glycosylation of the protected lactose derivative **11** with the known alcohol **12**.[55] **12** was then deprotected to yield **2b** (Figure 3).

The preparation of monomers **1b** and **2a** was achieved by alkylation of the aromatic units **16**[56] and **17**[57] using the iodide **15** obtained from the bromide **14**[58] by a Finkelstein halide exchange reaction. This iodide was then used to introduce a protected lactosyl unit in a single step (Figure 3).

The monomer **3** was prepared starting from 2,5-anhydromannitol. After a selective protection−deprotection sequence, the known diol

(45) Wataoka, I.; Kobayashi, K.; Kajiwara, K. *Carbohydr. Res.* **2005**, *340*, 989–995.
(46) Colin Hughes, R. *Biochimie* **2001**, *83*, 667–676.
(47) Danguy, A.; Camby, I.; Kiss, R. *Biochim. Biophys. Acta* **2002**, *1572*, 285–293.
(48) Miyagawa, A.; Kasuya, M. C. Z.; Hatanaka, K. *Carbohydr. Polym.* **2007**, *67*, 260–264.
(49) Choi, Y. H.; Liu, F.; Park, J. S.; Kim, S. W. *Bioconjugate Chem.* **1998**, *9*, 708–718.
(50) Hasegawa, T.; Umeda, M.; Matsumoto, T.; Numata, M.; Mizu, M.; Koumoto, K.; Sakurai, K.; Shinkai, S. *Chem. Commun.* **2004**, 382–383.
(51) Grosse, S.; Aron, Y.; Honoré, I.; Thévenot, G.; Danel, C.; Roche, A.-C.; Monsigny, M.; Fajac, I. *J. Gene Med.* **2004**, *6*, 345–356.
(52) Fleming, C.; Maldjian, A.; Da Costa, D.; Rullay, A. K.; Haddleton, D. M.; St. John, J.; Penny, P.; Noble, R. C.; Cameron, N. R.; Davis, B. G. *Nat. Chem. Biol.* **2005**, *1*, 270–274.
(53) Akamatsu, K.; Yamasaki, Y.; Nishikawa, M.; Takakura, Y.; Hashida, M. *Biochem. Pharmacol.* **2001**, *62*, 1531–1536.
(54) The synthesis and characterization of every new compound is detailed in the Supporting Information.
(55) Dickerson, T. J.; Reed, N. N.; Janda, K. D. *Bioorg. Med. Chem. Lett.* **2001**, *11*, 1507–1509.
(56) Henry, D. W.; Silverstein, R. M. *J. Org. Chem.* **1966**, *31*, 2391–2394.
(57) Patrick, D. A.; Boykin, D. W.; Wilson, W. D.; Tanious, F. A.; Spychala, J.; Bender, B. C.; Hall, J. E.; Dykstra, C. C.; Ohemeng, K. A.; Tidwell, R. R. *Eur. J. Med. Chem.* **1997**, *32*, 781–793.
(58) Davis, B. G.; Maughan, M. A. T.; Green, M. P.; Ullman, A.; Jones, J. B. *Tetrahedron: Asymmetry* **2000**, *11*, 245–262.

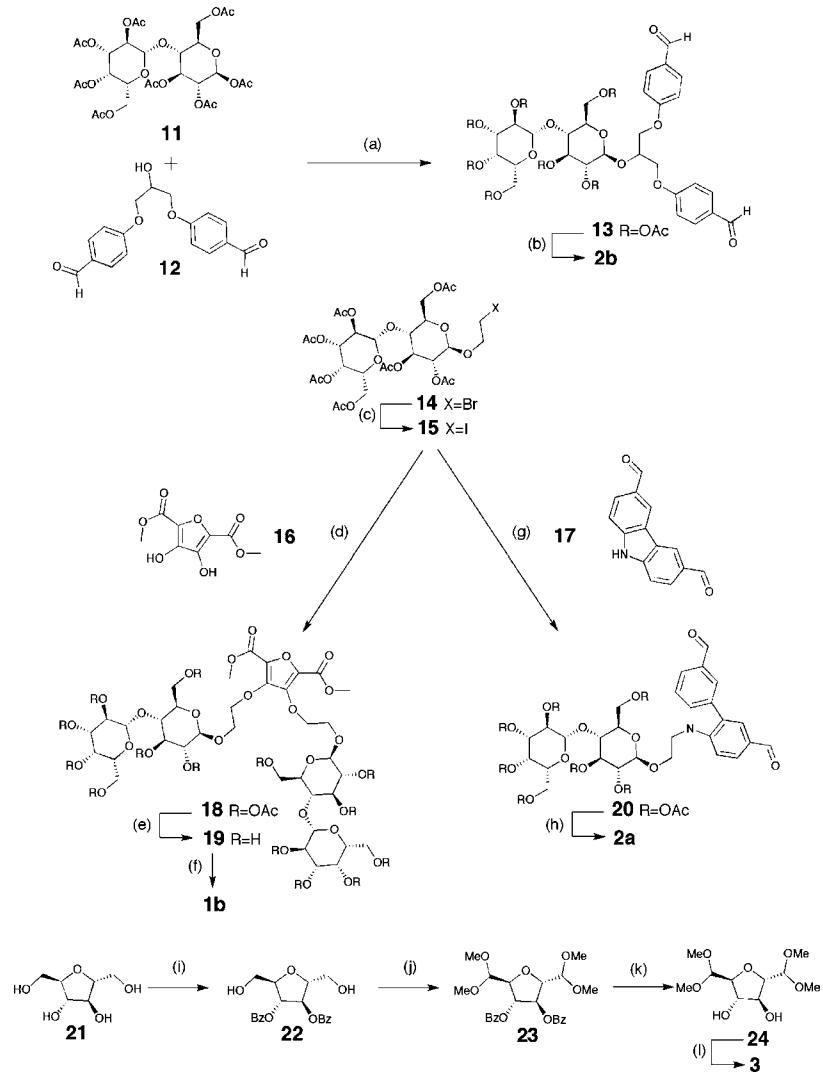

Figure 3. Synthesis of monomers **1b**, **2a**, **2b**: (a) BF_3OEt_2, CH_2Cl_2, reflux, the product was used directly for the next step; (b) NEt_3/MeOH/H_2O 8/58/24, 13% over two steps; (c) NaI, acetone, reflux; (d) K_2CO_3, 18-Crown-6, DMF, 40 °C, 48H, 79%; (e) KCN cat., MeOH, 77%; (f) NH_2NH_2 monohydrate, MeOH, 74%; (g) K_2CO_3, 18-Crown-6, DMF, 45 °C, 20H, 60%; (h) NEt_3/MeOH/H_2O 8/58/24, 76%; (i) (i) TrCl, pyridine, (ii) BzCl, pyridine, (iii) AcOH, H_2O; (j) (i) TEMPO, trichloroisocyanuric acid, (ii) $CH(OMe)_3$, MeOH, *p*-toluene sulfonic acid, 53% over two steps; (k) NaOMe, MeOH, 80%; (l) pD < 1, DCl, 50 °C, 24 h, D_2O, quant.

22[59] was oxidized, and the resulting aldehyde was protected as the dimethylacetal **23**. Removal of the benzoyl protecting groups yields **24**. The aliphatic dialdehyde **3** was obtained after hydrolysis of **24** (Figure 3).

NMR Spectroscopy. ^1H and ^{13}C NMR measurements were conducted on a Bruker Advance 400 MHz spectrometer. Chemical shifts are referenced with residual solvent signal (7.26 ppm, 77.16 ppm) in $CDCl_3$, ^{t}BuOH (1.24 ppm, 70.36 ppm, 30.29 ppm), or MeOH (3.34 ppm, 49.5 ppm) in D_2O.

Fluorescence Spectroscopy. Fluorescence measurements were done on a Jobin-Yvon Horiba Fluorolog 3.22 spectrometer.

Small-Angle Neutron Scattering (SANS). SANS experiments were carried out on the PACE spectrometer in the Léon Brillouin Laboratory at Saclay (LLB, France). The chosen incident wavelength, λ, depends on the set of experiments, as follows. For a given wavelength, the range of the amplitude of the transfer wave vector, q, was selected by changing the detector distance, D. Three sets of sample-to-detector distances and wavelengths were chosen (λ = 4.5 Å, D = 1 m; λ = 6 Å, D = 1.85 m; and λ = 13 Å, D = 4.67 m) so that the following q-ranges were respectively available: $4.23 \times 10^{-2} \le q \le 4.35 \times 10^{-1}$ Å^{-1}, $1.7 \times 10^{-2} \le q \le 1.79 \times 10^{-1}$ Å^{-1}, and $3.2 \times 10^{-3} \le q \le 3.4 \times 10^{-2}$ Å^{-1}. Measured intensities were calibrated to absolute values (cm^{-1}) using normalization by the attenuated direct beam classical method. Standard procedures to correct the data for the transmission, detector efficiency, and backgrounds (solvent, empty cell, electronic, and neutronic background) were carried out. The scattered wavevector, q, is defined by eq 1, where θ is the scattering angle.

$$q = \frac{4\pi}{\lambda} \sin \frac{\theta}{2} \tag{1}$$

The usual equation for absolute neutron scattering combines the intraparticle scattering $S_1(q) = V_{chain}\phi_{vol}P(q)$ form factor with the interparticle scattering $S_2(q)$ factor:

$$\begin{aligned} I(q)(\mathrm{cm}^{-1}) = \frac{1}{V}\frac{\mathrm{d}\sigma}{\mathrm{d}\Omega} &= (\Delta\rho)^2(S_1(q) + S_2(q)) \\ &= (\Delta\rho)^2(V_{chain}\phi_{vol}P(q) + S_2(q)) \end{aligned} \tag{2}$$

where $(\Delta\rho)^2 = (\rho_{monomer} - \rho_{solvent})^2$ is the contrast per unit volume between the polymer and the solvent, which was determined from the known chemical composition. $\rho = \sum n_i b_i / (\sum n_i m_i \upsilon \times 1.66 \times$

(59) Kuszmann, J.; Medgyes, G.; Boros, S. *Carbohydr. Res.* **2005**, *340*, 1739–1749.

10^{-24}) represents the scattering length per unit volume; b_i is the neutron scattering length of the species i, m_i is the mass of species i, and v is the specific volume of the monomer (which has been measured on a helium pycnometer for **1a** (0.629 cm^3/g) and **2b** (0.7 cm^3/g)) or the solvent (i.e., 0.9026 cm^3/g for D_2O). $P(q)$ is the form factor, $V_{chain} = Nvm \times 1.66 \times 10^{-24}$ is the volume of N monomers (of mass m) in a chain, and ϕ_{vol} is the volume fraction of monomer. In the high q-range, the scattering is assumed to arise from isolated chains, that is, $S_2(q) = 0$, and thus $I(q) \propto P(q)$.

GPC Measurements. GPC was performed on an Agilent 1100 Series GPC-SEC Analysis System equipped with three serial Shodex OH-pak (30 cm) columns (1803HQ, 1804HQ, 1806HQ) and a guard column. Detection was performed by a differential refractometer OPTILAB rEX (Wyatt Techn.) and a multi-angle light scattering detector DAWN HELEOS (Wyatt Techn). The injected volume was 100 mL. The flow rate was 0.5 mL/min, and the eluent was high-purity Millipore quality water containing 0.1 M $NaNO_3$ and NaN_3.

Cryo-TEM Analysis. Vitrified specimens for cryogenic-temperature transmission electron microscopy (Cryo-TEM) were prepared in a controlled environment vitrification system (CEVS) at 25 °C and 100% relative solvent saturation, as previously described.[60,61] In brief, a drop of the solution to be imaged was applied onto a perforated carbon film, supported on an electron microscopy copper grid, held by the CEVS tweezers. The sample was blotted by filter paper and immediately plunged into liquid nitrogen (−196 °C). The vitrified samples were then stored under liquid nitrogen, transferred to a Gatan 626 cooling holder via its "workstation", and kept in a FEI T12 G^2 microscope at about −180 °C. Images were recorded at 120 kV acceleration voltage, in the low-dose mode, to minimize electron-beam radiation-damage. We used a Gatan UltraScan 1000 high-resolution cooled-CCD camera, with the Digital Micrograph software package, to acquire the images. Images were recorded at nominal underfocus of about 1−2 μm to enhance phase contrast.

SPR Measurements. Surface plasmon resonance experiments were performed on a BIAcore 2000 (Biacore technology, Biacore AB, Uppsala, Sweden). The peanut agglutinin lectin was immobilized on the carboxylated sensor surface by a standard EDC (*N*-ethyl-*N*′-(3-dimethylaminopropyl)carbodiimide hydrochloride)/*N*-hydroxysuccinimide protocol. 10 and 20 μL of a PNA solution (100 μg mL^{-1}, 50 mM phosphate buffer pH = 6, 154 mM NaCl) were injected trough two of the chip channels, resulting in the immobilization of, respectively, 1408 and 3000 refractive unit (RU) of the protein on the surface. After immobilization, the remaining reactive activated carboxylic acids were capped with an ethanolamine solution.

Results and Discussion

Characterization of Glycopolymers 1a2a, 1a2b, 1b2a, 1b2b, and 1a3. A. NMR Characterization of the Glycopolymers. The five possible glycodynamers **1a2a**, **1a2b**, **1b2a**, **1b2b**, and **1a3** were obtained by polycondensation of a diluted solution of dialdehyde **2a**,**b** or **3** and dihydrazide **1a**,**b** monomers in D_2O (10 mM) under mild acidic conditions, typically pD = 4−6.

As the chemical shifts of imines proton signals are sensitive to small structural variations, it was hoped that each polymer would have a specific ^{1}H NMR signature in the imine region. Yet in all cases polymerization was associated with a dramatic broadening of the aromatic main chain signals, which may be interpreted in terms of a reduction of the mobility of these molecular segments in the polymeric structure (Figure 4). The proton NMR signals of the main chain are broadened beyond visibility, whereas those of the flexible saccharide side chains are still observable. This feature clearly indicated that the polycondensation and the expected micellar folding took place, but precluded the direct observation of imines signals that are generally well-defined individual singlets. Destabilization of hydrophobic forces should prevent the collapse of the hydrophobic main chain, which consequently should gain mobility, and therefore allow circumventing this problem. To achieve this "denaturation", we chose to use DMSO, an aprotic polar solvent, which, in principle, is able to dissolve both the lateral oligosaccharides chains and the aromatic core residues. Indeed, addition of d_6-DMSO to an aqueous solution of polymer **1a2b** allowed us to assign[62] and integrate all signals attributed to the aromatic main chain of the polymer. In the ^{1}H NMR spectrum (DMSO-d_6/D_2O 4/1) of the polymer **1a2b**, the signals corresponding to the imine (8.34 ppm), aromatic dialdehyde (7.71 and 7.04 ppm), and dihydrazide monomer (7.95 and 7.58 ppm) could be clearly assigned. No free monomer was detected (Figures 4 and 5). A similar behavior was observed for the polymers **1b2b** and **1a3**, suggesting for both of them a reversible micellar folding of the polymer backbone that can be circumvented by addition of DMSO.[63]

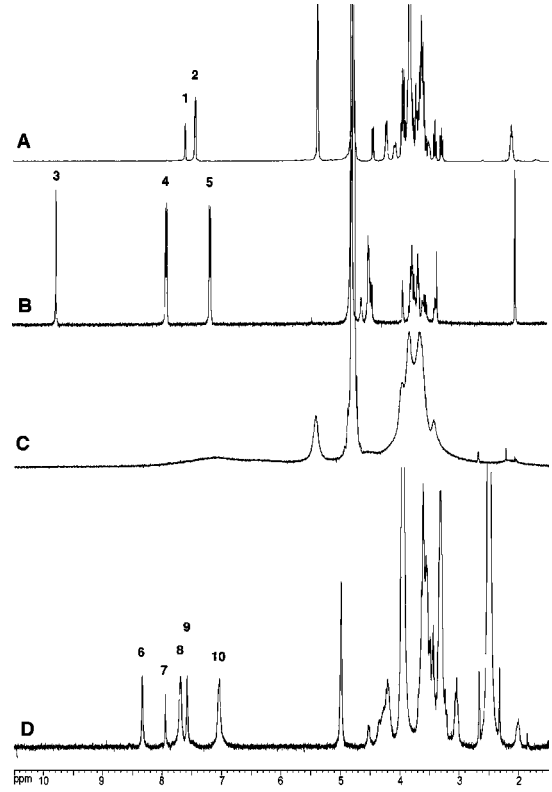

Figure 4. (A) ^{1}H NMR (D_2O, 400 MHz, 298 K) of monomer **1a**. (B) ^{1}H NMR (D_2O, 400 MHz, 298 K) of monomer **2b**. (C) ^{1}H NMR (D_2O, 400 MHz, 298 K) of polymer **1a2b** with an initial monomer concentration of 10 mM, at pD = 4. (D) ^{1}H NMR (DMSO-d_6/D_2O 5/1) obtained after dilution of 100 μL of the above polymer **1a2b** solution in 500 μL of DMSO-d_6. The proton numbering for signal attribution is shown in Figure 5.

B. Cryo-TEM. Evidence in favor of a cylindrical micelle-like conformation was provided by cryo-TEM images of polymer **1a2b** (Figure 6, left). This picture clearly shows thread-

(60) Talmon, Y. In *Modern Characterization Methods of Surfactant Systems*; Binks, B. P., Ed.; Dekker: New York: 1999; p 147.
(61) Bellare, J. R.; Davis, H. T.; Scriven, L. E.; Talmon, Y. *J. Electron Microsc. Technique* **1988**, *10*, 87–111.
(62) Complete assignation required 2D NMR experiments (COSY) and is given in the Supporting Information.
(63) The effect of addition of DMSO on the NMR spectrum of these polymers can be found in the Supporting Information.

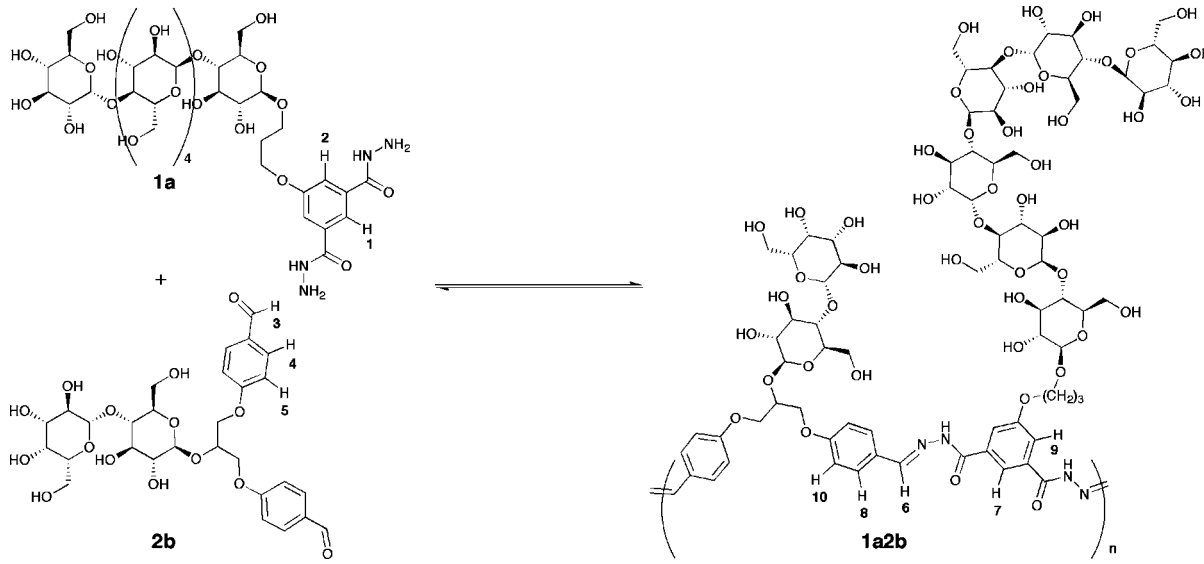

Figure 5. Preparation of the dynamic glycopolymer **1a2b** by polycondensation of monomers **1a** and **2b**. The corresponding proton NMR signals are shown in Figure 4.

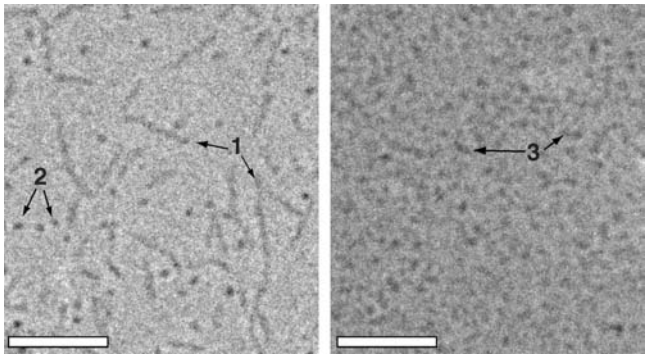

Figure 6. Left: Cryo-TEM image of a sample of polymer **1a2b** prepared in D_2O with an initial monomers concentration of 5 mM in the presence of a catalytic amount of *d*-TFA (5 mol %); **1**, typical individual polymeric filaments; **2**, spherical aggregates. Right: Cryo-TEM image of a sample of polymer **1a3** prepared in D_2O, with an initial monomers concentration of 10 mM at pD = 5; **3**, typical **1a3** ellipsoidal structures. The scale bars correspond to 50 nm.

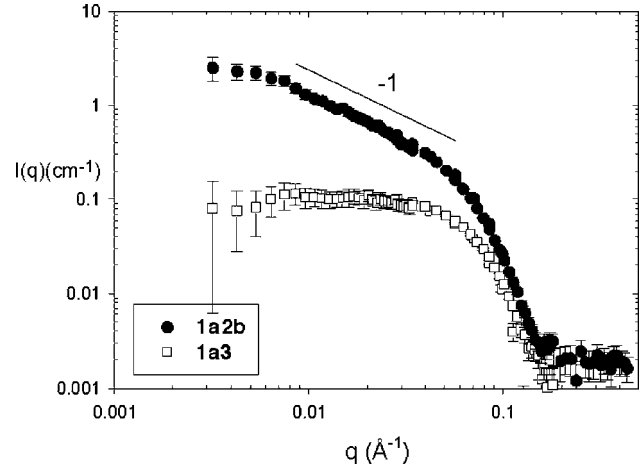

Figure 7. SANS scattered intensity as a function of *q* for polymer solutions **1a2b** and **1a3** at pD = 4 and 34 °C with an initial concentration of monomers of 5 mM.

like polymeric structures, in addition to small spheroidal entities that could correspond to either free monomers aggregated into small micelles or small cyclic oligomers. Some of these black dots are in fact polymer filaments with their longitudinal axis oriented perpendicular to the surface of the sample. Because of the thickness of the vitrified specimen, the length of the polymers is not accessible using this technique; it nevertheless provides a good approximation of the section of the polymer. The width of the filaments lies between 40 and 50 Å. As the length of the oligosaccharide residues in an extended conformation should be 2.8 nm for **1a**, and 1 nm for **2b**,[64] these dimensions are consistent with a honeycomb shape with the hydrophobic polymer main chain bristling with lateral oligosaccharide chains. In addition, these dimensions are in agreement with the expected diameter of a single polymer chain as reported for single polystyrene chains decorated with similar oligosaccharides side chains.[45]

The average diameter of the spherical aggregates is between 40 and 50 Å. As monomers **1a** and **2b** are amphiphilic molecules, this size could be consistent with the formation of micelles composed of residual monomers or small cyclic oligomers that would be present as traces in the polymerization mixture (these species were not detected by GPC,[65] confirming that their proportion is not significant). It is interesting to note that this bimodal distribution is unusual for equilibrium polymers.

For polymer **1a3** (Figure 6, right), the wormlike structures observed in the case of **1a2b** are absent, and only small ellipsoidal structures are observed. The average length of their longitudinal axis was measured to be 39 ± 5 Å, which is similar to that of **1a2b**, suggesting that, not unexpectedly, **1a** dominates the section of **1a3**.

C. Small-Angle Neutron Scattering. To characterize in more detail the conformation and length of the present type of dynamic glycopolymers, we performed small-angle neutron

(64) Values were determined using the commercial software Chem3D after energy minimization using the MM2 computation model.

(65) The GPC profiles can be found in the Supporting Information.

scattering (SANS)[66] on polymer **1a2b** and **1a3** equilibrated for 72 h. Figure 7 displays the scattering pattern obtained for these polymers. For **1a2b**, the scattering curve exhibits an overall behavior, characterized by the following sequence: a Guinier regime in the low-q range, associated with the finite size of the polymers, an intermediate regime in which the q-dependence of the scattered intensity can be described by a power law with an exponent equal to -1, followed by another Guinier regime associated with the cross-section of the supramolecular polymers. For polymers **1a3**, one observes only one Guinier regime associated with the mass and size of the system.

For polymer **1a2b**, the absence of q^{-2}-dependence of the scattered intensity $I(q)$, which would be characteristic of flexible wormlike chains, and the q^{-1}-dependence of $I(q)$ just after the Guinier regime indicate that this polymer may be considered a rigid rod. The low-q **1a2b** data corresponding to large spatial scales can be fitted by the following Guinier expression, giving the radius of gyration, R_g, of the polymer chains:

$$\frac{1}{I(q)} = \frac{1}{I(0)}\left(1 + \frac{q^2R_g^2}{3}\right) \tag{3}$$

From the best linear fit (see inset of Figure 9) to the data, one obtains $R_g = 187$ Å. The measurement of the radius of gyration, R_g, can be expressed as a function of L_p, using the Benoit−Doty expression derived for a wormlike chain of contour length, L, without excluded volume interactions.[67]

$$\langle R_g^2\rangle = \frac{LL_p}{3} - L_p^2 + \frac{2L_p^3}{L} - \frac{2L_p^4}{L^2}\left(1 - \exp\left(\frac{-L}{L_p}\right)\right) \tag{4}$$

For rodlike particles with large aspect ratio, the average contour length of the rod $L \ll L_p$, as shown by the cryo-TEM pictures and the intermediate q^{-1} regime. Expression (4) simplifies then to $R_g^2 = L^2/12$, giving L. In the case of polymer **1a2b**, one obtains $L = 65$ nm.

Neglecting the excluded volume interactions, the extrapolation to zero-q of the scattered intensity, $I(q^2 = 0)$, provides a measure of the weight-average molecular weigth of the polymers, $M_w = [I(q = 0) \times N_A]/[(\Delta\rho)^2 \times \phi_{vol} \times \upsilon]$, where $(\Delta\rho)^2$ is the contrast per unit volume between the polymer and the solvent, which was determined from the known chemical composition. N_A is Avogadro's number, ϕ_{vol} is the volume fraction of monomers, and υ is the specific volume of the monomer, which has been measured to 0.66 cm^3/g after determination of the density for monomers **1a** ($d = 1.59$) and **2b** ($d = 1.43$) on a helium pycnometer. The weight average molecular weight measured for the sample **1a2b** presented in Figure 9 is 511 000 g mol^{-1} corresponding to about 275 monomeric units with an initial monomer concentration of 5 mM at pD = 4, after 72 h of equilibration.

In the intermediate regime, $I(q)$ is controlled by smaller distances than L_p over which polymers **1a2b** are rodlike, and we observe a q^{-1}-dependence for the form factor $P(q)$, which is typical for locally rod structures. In this regime, where $I(q) \propto P(q)$, the data can be fitted by the des Cloizeaux expression:

$$P(q) = \frac{\pi}{qL} + \frac{2}{3q^2L_pL} \tag{5}$$

The fit shown in Figure 9 gives the following value for the linear density, $M_L = 744$ g/mol/Å. From values of M_w and M_L, one obtains the contour length of polymers **1a2b**: $L = M_w/M_L = 69$ nm, a value in excellent agreement with that of 65 nm obtained using the Benoit−Doty expression above.

For polymer **1a2b**, similar results were obtained for all temperatures and pD values investigated (Figure 8). As no temperature or time dependence of the molecular weight was observed by SANS experiments, the polymer **1a2b** can be considered as nondynamic at the time scale of these experiments (24 h). However, over a period of 4 months, the molecular weight of **1a2b** was found to evolve slowly toward higher masses by elongation of the individual polymer chains (see GPC data below).

Finally, the high-q data can be fitted by a Guinier expression for the form factor of the dynamic polymer section:

$$V_{chain}P(q) = \frac{\pi S}{q}\exp(-\frac{q^2R_c^2}{2}) \tag{6}$$

where R_c is the radius of gyration of the cross-section. By fitting the above equation to the experimental data, one can determine the cross-section, S, and the radius of gyration of the cross-section. From the fit of Figure 9, we obtain $S = 1300$ Å^2 and $R_c = 17.3$ Å for polymer **1a2b**. As polymer **1a2b** may be considered a solid cylinder, $d = \sqrt{8}R_c$, which gives a section diameter of 48.9 Å, in agreement with the cryo-TEM observations.

Similar SANS analyses were conducted on polymer **1a3**, yielding a radius of gyration, R_g, between 32 and 34 Å, with small variations with temperature and pH, whereas polymer **1a2b** showed no temperature dependence at all. It is thus much shorter than the 187 Å R_g measured for **1a2b**. In view of the cryo-TEM data, **1a** may be assumed to contribute mainly to the cross-section of the polymers **1a2b** and **1a3**, which should have similar cross-sections, so that an ellipsoidal model could be used to calculate the longitudinal length of **1a3**.

The radius of gyration, R_g, for an ellipsoid, with radii a, b, and c, and $b = c$ (ellipsoid of revolution), can be written:[68] $R^2_g = (b^2/5) \times (2 + a^2/b^2)$. Assuming that $b = d/2 = 24.5$ Å is identical for both polymers **1a3** and **1a2b**, we found $a = 61.9$ Å, that is, an axial ratio of ∼2.5 for **1a3**, explaining the absence of the q^{-1} regime.

Similar Guinier analysis and $I(q = 0)$ extrapolation gave an average molecular weight of 39 000 g mol^{-1} for **1a3**, at pD = 5, with an initial concentration of monomers of 5 mM, corresponding to 28 monomeric units.

D. Fluorescence Spectroscopy. In addition to SANS and cryo-TEM data, other results support the bottle-brush secondary structure of the polymers. Whereas among the monomers only **2a** was significantly fluorescent, all four polymers displayed remarkable fluorescence with a wide range of emission maxima from blue for **1a2b** ($\lambda_{max} = 457$ nm) to green for **1a2a** ($\lambda_{max} = 495$ nm), **1b2b** ($\lambda_{max} = 499$ nm), and to red for **1b2a** ($\lambda_{max} = 567$ nm) (Figure 10, Table 1).

These fluorescence properties are likely to result from the tightly packed structure of the polymer, where aromatic chromophores are isolated in the hydrophobic core and rigidly held,

(66) Buhler, E.; Candau, S. J.; Schmidt, J.; Talmon, Y.; Kolomiets, E.; Lehn, J.-M. *J. Polym. Sci., Part B: Polym. Phys.* **2007**, *45*, 103–115.
(67) Benoit, H.; Doty, P. *J. Phys. Chem.* **1953**, *57*, 958–963.
(68) Guinier, A.; Fournet, G. *Small-Angle Scattering of X-rays*; John Wiley and Sons: New York, 1955.

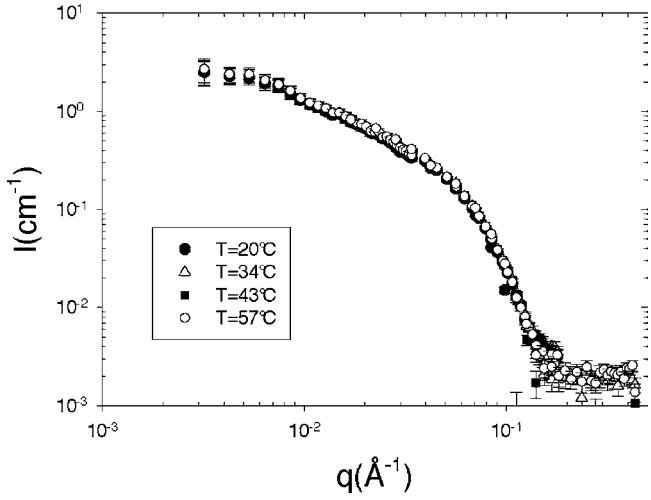

Figure 8. Effect of the temperature on the small-angle neutron scattering patterns for polymers **1a2b** at a monomer concentration of 5 mM and pD = 4.

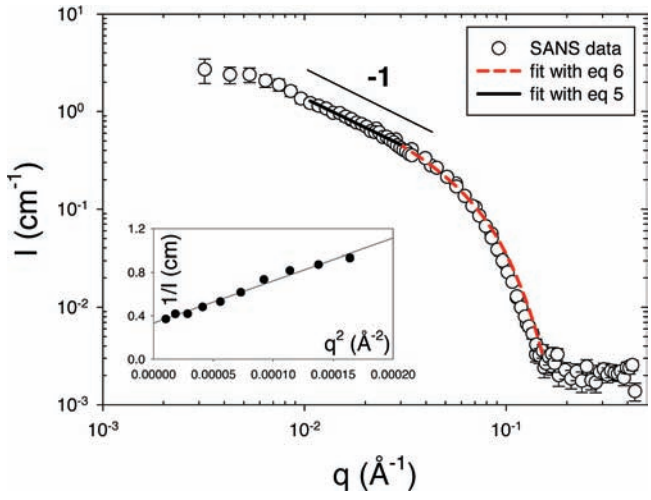

Figure 9. SANS spectra obtained for a 5 mM solution of **1a2b** in D_2O at $T = 57$ °C and pD = 4. The black line represents the fit of the data in the intermediate regime with eq 5, and the dashed red line represents the fit of the high q data by a Guinier expression for the form factor of the section (eq 6). The linear correlation between $I(q)^{-1}$ and q^2 is represented in the inset.

preventing nonradiative decay processes. Therefore, the collapse of the aromatic units of polymer backbone during the formation of the cylindrical micellar structure resulted in a dramatic increase in their fluorescence emission efficiency. Such aggregation-induced emission enhancement (AIEE)[69,70] phenomena have already been reported for different aromatic systems and have been attributed in particular to the restriction of intramolecular rotations. In our case, we can therefore imagine a similar scenario, where the reduction of the intramolecular rotations of the conjugated aromatic hydrazones units of the polymer backbone would result in an increase in fluorescence emission of these fluorophores. The contribution of stacking interactions (H- or J-type) could also be considered,[71−73] as reported for isophthalic acid bis-amide derivatives,[73] a structural

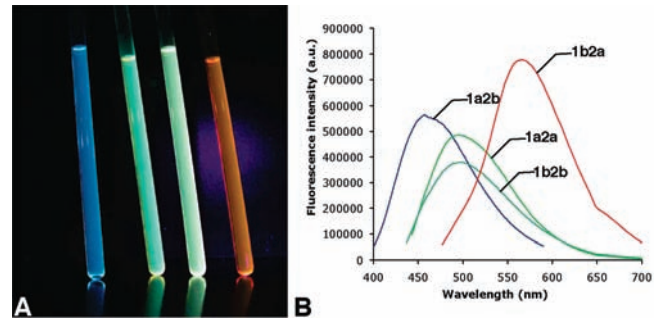

Figure 10. (A) Photography of samples of the polymers **1a2b**, **1a2a**, **1b2b**, and **1b2a** under UV irradiation (365 nm) in D_2O at pD = 4 with an initial monomer concentration of 5 mM; (B) emission spectrum of the same polymer samples (for polymer **1b2a**, a slit width of 3 nm was used instead of 1 nm for the others) irradiated at their respective maximum for excitation. The excitation maxima are given in Table 1, and the excitation spectra are shown in the Supporting Information.

Table 1. Optimal Wavelength for the Excitation ($\lambda^{max\ ex}$) and Emission ($\lambda^{max\ em}$) of Glycopolymers **1a2a**, **1a2b**, **1b2a**, and **1b2b**[a]

	1a2a	1a2b	1b2b	1b2a
$\lambda^{max\ ex}$ (nm)	433	389	427	467
$\lambda^{max\ em}$ (nm)	495	457	499	567

[a] Samples were prepared in D_2O at pD = 4 with an initial monomer concentration of 5 mM.

unit found in monomer **1a**. For polymer **1a2b**, the fluorescence intensity decreases markedly upon addition of DMSO to the polymer solution, presumably due to the destabilization of the highly packed structure (Figure 11), further supporting the influence of intramolecular motions and presumably stacking interactions in the fluorescence properties of our polyhydrazones.[74] The decrease in fluorescence intensity upon heating also suggests an increase in molecular motion of the conjugated aromatic core of the polymer. This phenomenon is well-known for fluorophores and usually results in a loss of fluorescence of 1% when the temperature increases by 1 °C.[75] However, in our case, the nonlinear dependence between the fluorescence intensity and the temperature suggests that an additional phenomenon such as a denaturation or change in conformation occurs.

E. GPC Measurements. GPC measurements were conducted using water as solvent. Table 2 is a compilation of results obtained for **1a2a**, **1a2b**, **1b2a**, and **1b2b** for samples equilibrated on different time scales.

Polymers **1a2a** and **1a2b** display very high molecular weights (>500 000 g/mol), which is already an interesting property, considering the facile preparation procedure of these water-soluble glycopolymers. Their radius of gyration, R_g, was measured by light scattering at the output of the GPC column and plotted against the determined molecular weight. A perfectly linear dependence was observed in both cases, confirming their rodlike character as $R_g = L/\sqrt{12}$ for rigid rodlike chains (Figure 12).

(69) Luo, J.; Xie, Z.; Lam, J. W. Y.; Cheng, L.; Chen, H.; Qiu, C.; Kwok, H. S.; Zhan, X.; Liu, Y.; Zhu, D.; Tang, B. Z. *Chem. Commun.* **2001**, 1740–1741.
(70) Hong, Y.; Lam, J. W. Y.; Tang, B. Z. *Chem. Commun.* **2009**, 4332–4353.
(71) Zhou, T.; Li, F.; Fan, Y.; Song, W.; Mu, X.; Zhang, H.; Wang, Y. *Chem. Commun.* **2009**, 3199–3201.
(72) Rabinowitch, E.; Epstein, L. F. *J. Am. Chem. Soc.* **2002**, *63*, 69–78.
(73) Qian, Y.; Li, S.; Zhang, G.; Wang, Q.; Wang, S.; Xu, H.; Li, C.; Li, Y.; Yang, G. *J. Phys. Chem. B* **2007**, *111*, 5861–5868.
(74) Shimojo, S.; Cho, C.-S.; Park, I.-K.; Kunou, M.; Goto, M.; Akaike, T. *Carbohydr. Res.* **2003**, *338*, 2129–2133.
(75) Guilbault, G. G. *Practical Fluorescence*, 2nd ed.; Marcel Dekker Inc.: New York, 1990; pp 28−29.

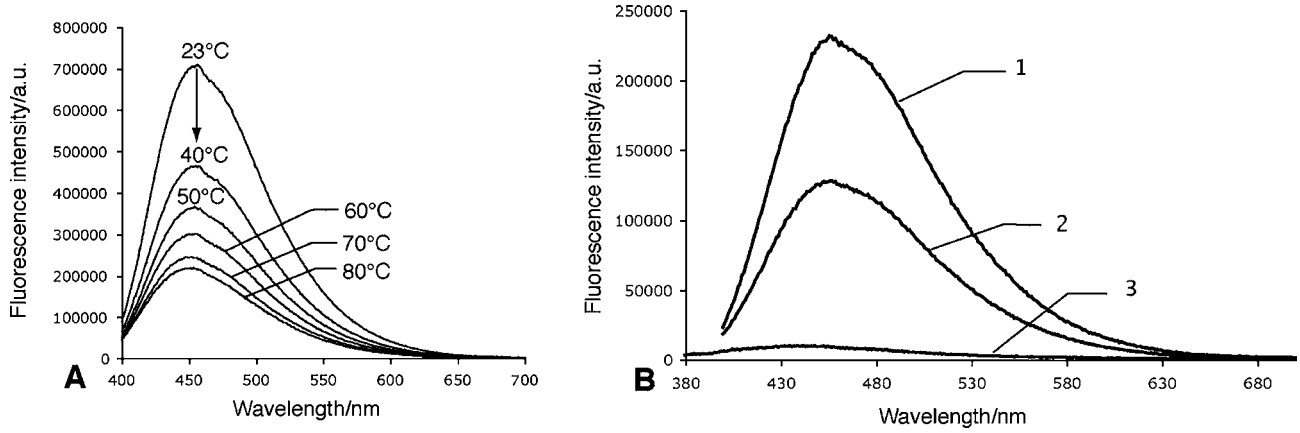

Figure 11. (A) Effect of temperature on the fluorescence intensity of a sample of **1a2b** in D_2O, at pD = 4 with an initial monomer concentration of 5 mM. (B) Effect of DMSO addition on the fluorescence intensity of a sample of **1a2b** (1) in D_2O, at pD = 4 with an initial monomer concentration of 5 mM; (2) after dilution of this solution (100 μL) in D_2O (500 μL); and (3) after dilution of this solution (100 μL) in DMSO-d_6 (500 μL).

Table 2. GPC Determination of the Molecular Weight of Glycopolymers **1a2a**, **1a2b**, **1b2a**, and **1b2b**[a]

	1a2a	1a2b	1b2b	1b2a
M_w (g mol^{-1})	1.38×10^6	1.76×10^6	4.93×10^4	3.32×10^4
M_n (g mol^{-1})	6.45×10^5	5.93×10^5	3.74×10^4	3.10×10^4
M_w/M_n	2.15	2.96	1.31	1.07

[a] Samples were prepared in D_2O at pD = 4 with an initial monomer concentration of 5 mM.

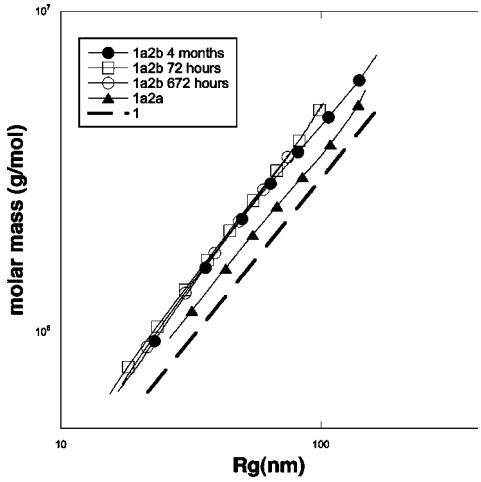

Figure 12. Linear relations between the molecular mass and the radius of gyration of polymers **1a2a**, equilibrated 4 months, and **1a2b** for samples equilibrated 4 months, 672 h, and 72 h, as determined by light scattering analysis of the GPC fractions.

Another feature of these dynamic polymers is that their "living" character drives the polymerization toward the formation of increasingly long polymers over time. Indeed, after 4 months of equilibration, polymer **1a2b** reached a molecular weight of 1.76×10^6, whereas after 72 and 672 h of equilibration, the observed M_w was 8.45×10^5 and 1.28×10^6 g mol^{-1}, respectively. Thus, the molecular weight, and therefore the length of this polymer, is time dependent. Within the experimental error bar, the overlap of the dependence between R_g and M_w for these three samples confirms a linear growth and rules out the possibility of lateral aggregation (Figure 12). This can be explained by considering that under the conditions of equilibration, the polycondensation reaction can still take place, and even if free monomers are absent, the reactive chain-end hydrazide or aldehyde is still able to form the hydrazone linkage. The living character of the polycondensation could also explain the low polydispersities observed for polymers **1b2a** (1.07) and **1b2b** (1.31). It has been shown that low polydispersity can be achieved by polycondensation if the polymerization has a living character and proceeds through a chain growth mechanism.[76] This approach was used to prepare polymers having polydispersity lower than 1.1, when classical step growth polycondensation yields polymers having polydispersities closer to 2,[77] as observed in our case for polymers **1a2a** and **1a2b**. The difference in polydispersity between polymers derived from **1a** or **1b** could then result from a different polymerization mechanism. Such a difference could result from a particular folding or conformation, possibly helicoidal,[78] of the main chain of polymers **1b2a** and **1b2b**, which would induce a strong cooperative polymerization, making the chain elongation faster and more favorable than the initiation of the growth of new polymer chains by the condensation of monomers.[78,79] This hypothesis is supported by the fact that even the addition of DMSO was not able to unfold the polymer main chain for **1b2a**.[80]

The difference between the M_w values determined for **1a2b** by GPC and SANS could be due to the fact that the analysis of GPC results implied the use of a d*n*/d*c* value, which was not measured but taken arbitrarily. SANS does not require this approximation and is therefore believed to be more accurate in the present case.

^{1}H NMR Study of the Dynamic Character of Polymer 1a2b. Demonstration of the dynamic character of the present glycopolymers was achieved by adding an equimolar amount of the dihydrazide monomer **1b** to the polymer **1a2b**, and monitoring its incorporation into the backbone of the polymeric structure using ^{1}H NMR (Figures 13 and 14).

The proton signals corresponding to the aromatic region of the polymer are extremely broad, but, as during exchange **1b** replace **1a** in the polymer, the release of the latter in solution was indicated by the appearance of sharp peaks for its aromatic and anomeric protons (Figure 13).

(76) Yokozawa, T.; Yokoyama, A. *Prog. Polym. Sci.* **2007**, *32*, 147–172.
(77) Flory, P. J. *J. Am. Chem. Soc.* **1936**, *58*, 1877–1885.
(78) Folmer-Andersen, J. F.; Lehn, J.-M. *Angew. Chem., Int. Ed.* **2009**, *48*, 7664–7667.
(79) Zhao, D.; Moore, J. S. *Org. Biomol. Chem.* **2003**, *1*, 3471–3491.
(80) The effect of addition of DMSO on the NMR spectrum of this polymer can be found in the Supporting Information.

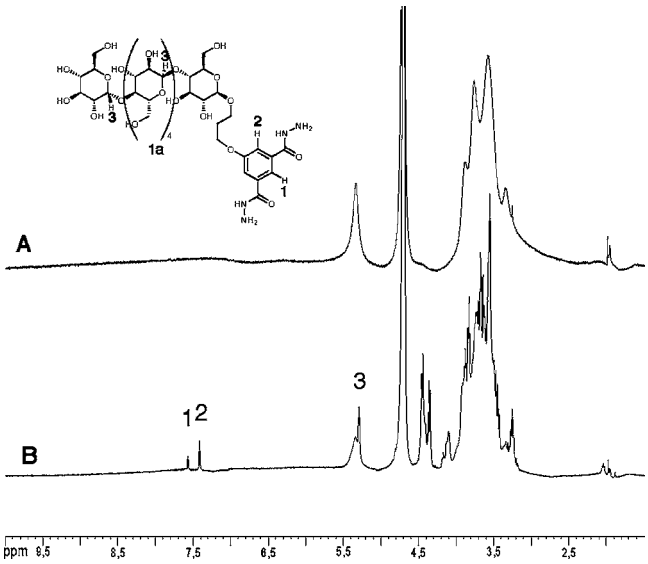

Figure 13. Part of the ^{1}H NMR spectra of a mixture of a solution of polymer **1a2b** in pD = 4 buffered D_2O, (A) before and (B) after addition of 1 equiv of **1b** and heating at 80 °C for 70 min. 1,2,3 designate the aromatic (1,2) and anomeric (3) signals of **1a** released from **1a2b** due to the incorporation of **1b**.

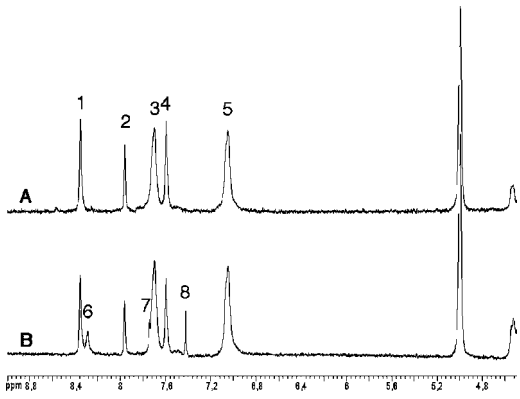

Figure 14. Part of the ^{1}H NMR spectra of a mixture obtained by dilution of 100 μL of a solution of polymer **1a2b** with 500 μL of DMSO-d_6, (A) before and (B) after addition of 1 equiv of **1b**. The signals 1−5 correspond to the polymer **1a2b** and 6−8 to **1a** released after exchange. Signals 1 and 6 are due to the imines protons, respectively, before and after exchange.

To be able to assign and integrate the aromatic and imine signals, the aqueous polymer solution was diluted 6 times in DMSO-d_6 before recording the ^{1}H NMR spectrum (Figure 14). Comparing the spectra of the polymer **1a2b** in DMSO-d_6/D_2O 5/1 before and after exchange with 1 equiv of **1b** allowed one to observe and quantify by integration the release of the initial dihydrazide **1a** from the polymeric structure. The appearance of two singlets corresponding to the signals of aromatic protons of the free dihydrazide **1a** (Figure 14, signals 7 and 8) and the emergence of a new imine signal (Figure 14, signal 6) confirm the incorporation of **1b** in the polymer. The half-time for exchange was 90 min and 25 h at 80 °C and room temperature, respectively, at pD = 4 with an initial monomer concentration of 5 mM. At pD = 7, no trace of exchange was detected even after 3 weeks at room temperature.

This incorporation of **1b** into polymer **1a2b** results in a modification of the polymer constitution.

Fluorescence Study of Chemical Exchange Reaction on 1a2b. It is also possible to follow the exchange reaction between **1a2b** and **1b** by fluorescence spectroscopy. Figure 15 shows the evolution of the fluorescence spectrum of polymer **1a2b** mixed with an equivalent of dihydrazide monomer **1b**. The emission maximum shifts from blue to green due to the incorporation of the new dihydrazide **1b** building block into the polymer, transforming progressively the polymer constitution from **1a2b** into **1a1b2b**, containing increasing amounts of **1b** at the expense of **1a** (see also Figure 10 and text).

It is of interest to note that these component exchange features together with the wide range of emission wavelengths (see above) suggest the possibility to modulate and tune the fluorescent properties of the system via the introduction of various components into the dynamic main chain. One may imagine a number of applications of such optodynamers[14] as adaptive fluorescent probes and effector responsive optical materials.

Improvement of Covalent Exchange Kinetics. Implementation of the adaptive character of these dynamic polymers for biological applications would require finding milder conditions for the covalent exchange reactions, with exchange half times in the order of hours or less at room temperature. To achieve this goal, we chose to decrease the formation efficiency of the imine linkage by using the strongly hydrated dialdehyde monomer **3**.

The polymer **1a3** was prepared from equimolar amounts of **1a** and **3** (5 mM each pD = 4). It had a fluorescence profile similar to that of **1a2b** with λ_{max} = 444 nm for emission and 383 nm for excitation.

As for the **1a2b** polymer, the reversible character of **1a3** was demonstrated by adding 1 equiv of the dihydrazide **1b** to its equilibrated form in aqueous solution and following the covalent exchange reaction by ^{1}H NMR (Figure 16).

The release of free **1a** was again observed and quantified by integration of the signal corresponding to its two equivalent aromatic protons in DMSO-d_6/D_2O 5/1 (Figure 16). The half-life for exchange at pD = 6 was 34 and 12 min at pD = 5 at room temperature with an initial concentration of monomers of 10 mM, that is, about 125 times faster than in the case of **1a2b** at pD = 4.

The incorporation of **1b** into the polymers **1a2b** and **1a3** demonstrates their dynamic nature and results in a modification of their constitution, which markedly affects their structural and functional properties.

Lectin Binding Properties of the Glycodynamers. Surface plasmon resonance (SPR) is a valuable tool for the rapid determination of kinetic and thermodynamic binding parameters between molecules or macromolecules, especially between carbohydrates and lectins.[81] After immobilization of the protein of interest on a surface, the potential ligand is allowed to interact with the receptor as its solution flows over the surface. The refractive index of the surface changes according to the mass of molecules bound to the surface and the receptor and can therefore be used to quantify the binding efficiency.

We used peanut agglutinin, PNA, as a model lectin for the preliminary investigations of the biological properties of our polymers, because of its specificity for β-galactose ligands, and especially for lactosyl units present in monomers **1b**, **2a**, and **2b**.[82,83]

(81) Duverger, E.; Frison, N.; Roche, A.-C.; Monsigny, M. *Biochimie* **2003**, *85*, 167–179.
(82) Natchiar, S. K.; Suguna, K.; Surolia, A.; Vijayan, M. *Crystallogr. Rev.* **2007**, *13*, 3–28.

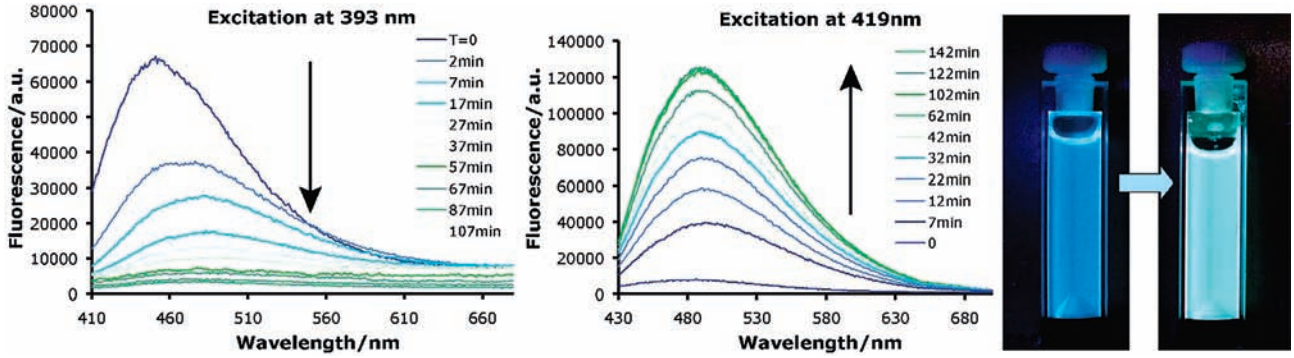

Figure 15. Left and center: Evolution of the fluorescence of **1a2b** after addition of **1b** under excitation at 393 and 419 nm. Right: Photography of samples of polymer **1a2b** before (left fluorescence cell) and after chemical exchange with **1b** (right fluorescence cell).

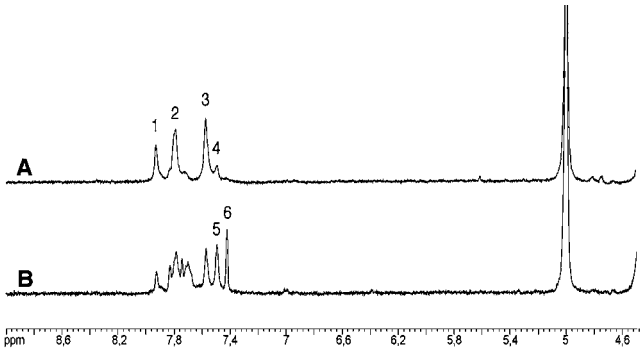

Figure 16. Part of the ^{1}H NMR spectra of a mixture obtained by diluting 100 μL of a solution of polymer **1a3** with 500 μL of DMSO-d_6, (A) before and (B) after addition of 1 equiv of **1b**. Signals 1−3 correspond to the polymer **1a3**, and signal 6 corresponds to the two equivalent aromatic protons of released **1a**. Signals 4 and 5 are due to the terminal monoimine of **1a**.

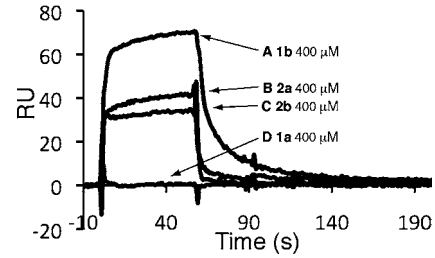

Figure 17. SPR sensograms resulting from interactions between PNA immobilized on a carboxylated surface (3000 RU) and (A) a solution of **1b** at 400 μM; (B) a solution of **2a** at 400 μM; (C) a solution of **2b** at 400 μM; and (D) a solution of **1a** at 400 μM. All samples were prepared in a phosphate buffer (50 mM) at pH = 6 containing NaCl (154 mM).

It was of particular interest to compare the SPR response of the monomers and of the corresponding polymers, to see whether the known glycocluster effect[23] and an increase in affinity would be observed.

The binding constants between PNA and monomers **1a**, **1b**, **2a**, and **2b** have been determined after SPR data fitting using the standard BIA evaluation software.

As expected from the PNA specificity, only monomers **1b**, **2a**, and **2b** induced significant response by SPR, giving equilibrium association constants K_A between 2 and 4 × 10^3 M^{-1} (for **1b**, $K_A = 2 \times 10^4$ M^{-1}; for **2a**, $K_A = 2.6 \times 10^3$ M^{-1}; for **2b**, $K_A = 3.8 \times 10^3$ M^{-1}). Interestingly, the bivalent monomer **1b** has an association constant for PNA, respectively, 7.7 and 5.2 times higher than the monovalent monomers **2a** and **2b**. This could be explained by the cluster glycoside effect, which is commonly observed for polyvalent carbohydrates ligands when compared to their monovalent counterparts for the same receptor.[23,84]

Monomer **1a** did not induce any significant response by SPR, and therefore polymer **1a3** showed no affinity for PNA (Figures 17 and 18).

Among the polymers, only polymers **1b2a** and **1b2b** induced a strong response by SPR, whereas polymers **1a2a**, **1a2b**, despite their high molecular weight, did not show a response higher than their corresponding monomers (Figure 18).

Thus, the maximum SPR response for **1a2a** was 10 RU (refractive unit), a value that has to be compared to the 517 RU measured for **1b2a** under the same experimental conditions. These results suggest that there is no significant affinity improvement of **1a2a** and **1a2b** for PNA with respect to the starting monomers. This behavior can be explained by the steric hindrance caused by the long maltohexaose side chains, which could prevent the lactosyl moieties present on monomers **2a** and **2b** from interacting with the PNA. In a way, lactosyl moieties are hidden by the long brushes that decorate the polymer.

Interestingly, the SPR response of polymers **1b2a** and **1b2b** is, respectively, 3.8 and 7.8 times higher than that induced by the starting monomers injected at the same concentration before polymerization takes place (Figure 18). Indeed, polymerization is slow in the experimental conditions used for SPR (pH = 6). Therefore, polymers **1a2a** and **1b2b** are markedly more effective ligands for PNA than are the corresponding monomers. A decrease of the dissociation rate, which is a common feature for multivalent glycopolymers, was also observed, but was difficult to quantify due to the multivalent nature of the interactions studied and to the dynamic character of our polymer that might dissociate to some extent upon dilution during the experiment. A complete study of the affinity of these polymers for lectins and of the effect of lectin binding on the molecular weight of these polymers would be of interest.

Conclusions

Dynamic analogues of glycopolymers have been generated using reversible acylhydrazone formation. Their dynamic character was demonstrated by covalent exchange reaction of a monomeric component by another, resulting in modification of the glycodynamer fluorescence properties. The molecular weight

(83) Jimbo, A.; Matsumoto, I. *J. Biochem.* **1982**, *91*, 945–951.
(84) Lee, Y. C.; Lee, R. T. *Acc. Chem. Res.* **1995**, *28*, 321–327.

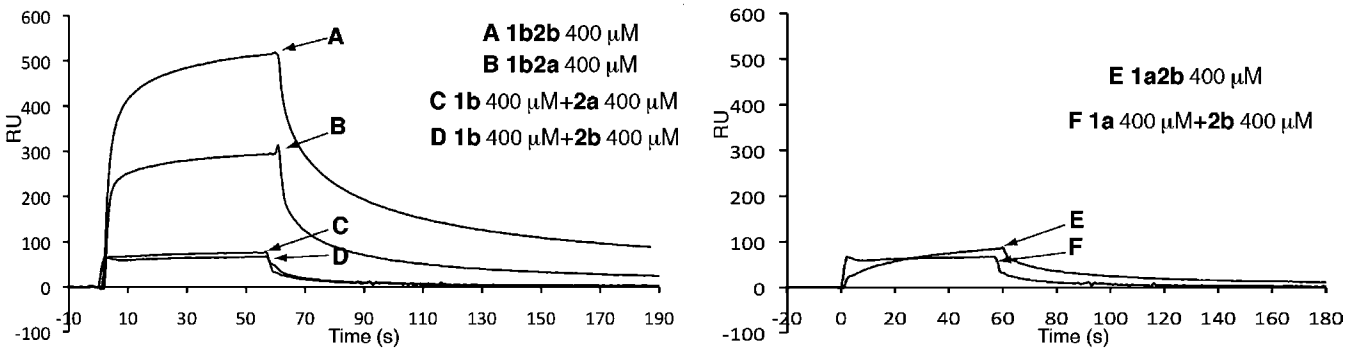

Figure 18. SPR sensograms resulting from interactions between PNA immobilized on a carboxylated surface (3000 RU) and (A) polymer **1b2b** solution prepared by diluting a solution with an initial monomer concentration of 5 mM to 400 μM; (B) polymer **1b2a** solution prepared by diluting a solution with an initial monomer concentration of 5 mM to 400 μM; (C) a mixture of monomers **1b** and **2a** both at 400 μM; (D) a mixture of monomers **1b** and **2b** both at 400 μM; (E) polymer **1a2a** solution prepared by diluting a solution with an initial monomer concentration of 5 mM to 400 μM; and (F) a mixture of monomers **1a** and **2b** both at 400 μM. All samples were prepared just before the analysis in a phosphate buffer (50 mM) at pH = 6 containing NaCl (154 mM).

as well as the rate of exchange were tuned by modification of the dialdehyde monomers. Dihydrazide monomers in combination with aromatic dialdehydes yield high molecular weight glycopolymers showing reversibility under rather drastic conditions, but stability under physiological conditions. This type of dynamer may be of interest for applications where slow decomposition is preferable, such as slow release of a drug. The use of the aliphatic dialdehyde **3** confers reversibility under milder conditions, yielding dynamers with a lower molecular weight, more susceptible to be of use for adaptive purposes, like multivalent templating with cell or bacteria receptors. Furthermore, the present fluorescent dynamic glycopolymers could have applications, in biotechnology for biosensing,[85] lectin,[86,87] bacteria,[87−89] toxin,[48] virus[88] binding, or labeling, in analytical chemistry for (adaptive) selective probes, for instance for heavy metal detection,[90] and in materials science for the development of species, such as polymeric films, presenting responsive optical properties.[91]

The preliminary investigations of the affinity of the present glycodynamers for PNA suggest that polymers **1b2b** and **1b2a** are more efficient ligands than the corresponding monomers. These experiments also revealed the detrimental effect of **1a** on binding to PNA, as **1a2a** and **1a2b** are only weak ligands. Therefore, not only the physicochemical properties, such as the fluorescence, but also the affinity for a biological target are, in principle, tunable by dynamic covalent exchange and modification of the polymer constitution through component exchange.

Finally, the results obtained extend the application of constitutional dynamic chemistry from materials science to biopolymers and illustrate some aspects of the potential of such biodynamers.

Acknowledgment. We wish to dedicate this work to the memory of Henri Benoît (deceased March 23rd, 2009). We thank the Ministère de la Jeunesse, de l'Education nationale et de la Recherche and the Collège de France for predoctoral fellowships to Y.R., as well as the Collège de France, the CNRS (UMR 7006) and the Université de Strasbourg for financial support.

Supporting Information Available: Experimental details for the synthesis and characterization of all new compounds and intermediates. Experimental details for the preparation of dynamic glycopolymers. Assignment of ^{1}H NMR signals of polymer **1a2b** and exchange reaction mixture **1a2b**+**1b** in DMSO-d_6/D_2O 5/1 using a 2D ^{1}H NMR COSY experiment. Effect of the dilution with DMSO on the main-chain mobility by ^{1}H NMR. GPC traces for polymers **1a2a**, **1a2b**, **1b2a**, and **1b2b**. Excitation and emission spectra for all polymers. This material is available free of charge via the Internet at http://pubs.acs.org.

JA9082733

(85) Jelinek, R.; Kolusheva, S. *Chem. Rev.* **2004**, *104*, 5987–6016.
(86) Kim, I.-B.; Wilson, J. N.; Bunz, U. H. F. *Chem. Commun.* **2005**, 1273–1275.
(87) Xue, C.; Jog, S. P.; Murthy, P.; Liu, H. *Biomacromolecules* **2006**, *7*, 2470–2474.
(88) Baek, M.-G.; Stevens, R. C.; Charych, D. H. *Bioconjugate Chem.* **2000**, *11*, 777–788.
(89) Disney, M. D.; Zheng, J.; Swager, T. M.; Seeberger, P. H. *J. Am. Chem. Soc.* **2004**, *126*, 13343–13346.
(90) Kim, I.-B.; Erdogan, B.; Wilson, J. N.; Bunz, U. H. F. *Chem.-Eur. J.* **2004**, *10*, 6247–6254.
(91) Abbel, R.; Grenier, C.; Pouderoijen, M. J.; Stouwdam, J. W.; Leclèıre, P. E. L. G.; Sijbesma, R. P.; Meijer, E. W.; Schenning, A. P. H. J. *J. Am. Chem. Soc.* **2008**, *131*, 833–843.